https://doi.org/10.5194/se-2020-53
Preprint. Discussion started: 14 May 2020
© Author(s) 2020. CC BY 4.0 License.

Solid Earth
Discussions
Open Access
EGU

Resolving uncertainties in the application of zircon Th/U and CL gauges to interpret U-Pb ages: a case study of eclogites in polymetamorphic terranes of NW Iberia

Pedro Castiñeiras[1], Juan Gómez Barreiro[2], Francisco J. Fernández[3], Carmen Aguilar[4] and José Manuel Benítez Pérez[5]

[1]Departamento de Petrología y Geoquímica, Universidad Complutense de Madrid, José Antonio Novais 12, 28040 Madrid (Spain).

[2]Departamento de Geología. Universidad de Salamanca. Facultad de Ciencias, Pza. de los Caidos s/n, 37008 Salamanca (Spain).

[3]Departamento de Geología., Universidad de Oviedo, Jesús Arias de Velasco s/n, 33005 Oviedo (Spain).

[4]Centre for Lithospheric Research, Czech Geological Survey, Klárov 3, 11821 Prague, Czech Republic.

[5]Centro de Ciências e Tecnologias Nucleares. Instituto Superior Técnico. Universidad de Lisboa. Estrada Nacional 10 (km 139,7), 2695-066, Bobadela LRS, Portugal

Correspondence to: J. Gómez Barreiro (jugb@usal.es)

castigar@ucm.es
brojos@geol.uniovi.es
carmen.gil@geology.cz
jose.benitez@ctn.tecnico.ulisboa.pt

Abstract. Zircon crystal texture and Th/U ratio have been used as a watertight argument when interpreting U-Pb ages. The wide, and sometimes indiscriminate, use of those gauges could result into misinterpretation of the geological meaning of U-Pb data. A case study is presented here where zircons from a controversial polymetamorphic eclogite unit were analyzed with SHRIMP. Both U-Pb and trace element (TE) data were collected for each point. The combination of TE and structural arguments indicates that zircon was part of the eclogite facies mineral assemblage at 390 Ma. However, using Th/U ratio and CL textures lead to a different interpretation. Our results suggest that in complex orogenic scenarios and extreme environments well-known techniques (CL) and geochemical relationships (Th/U) must be used in combination with TE data and structural relationships as provenance/process gauges. While geochronology provides accurate isotope relationships, their temporal dimension must rely on structural and petrological evidence.

1 Introduction

https://doi.org/10.5194/se-2020-53
Preprint. Discussion started: 14 May 2020
© Author(s) 2020. CC BY 4.0 License.


Dating metamorphic rocks using the U-Pb isotopic system in zircon can be a challenging task owing to the ability of this mineral to grow in a variety of geological conditions and its relative resistance to metamorphic processes. When the evolution of a rock results in complex textures in zircon, the combination of the high spatial resolution provided by the SIMS (secondary ionization mass spectrometry) instruments together with cathodoluminescence (CL) or backscattered (BS) images has turn out to be very convenient in most cases to decipher this intricate history (see Corfu et al., 2003). As most of the geological processes result in a specific set of zircon textures under CL or BS, this methodology strongly relies in our ability to recognize the origin of zircon based on those textures, so we can link the obtained ages to specific geological processes. For example, the most frequent texture in metamorphic zircon is homogeneous zoning found in discordant rims (Rubatto and Gebauer, 2000), patchy zoning is commonly found in eclogitic zircon (Tomaschek et al., 2003), soccer-ball zoning appears in high-grade metamorphic rocks (Fernández Suárez et al., 2007), subrounded and truncated internal areas are considered inherited zircon (xenocrystic cores), and oscillatory zoning is typical of magmatic zircon (Corfu et al., 2003). However, there is a lack of understanding of the zircon growth process, precluding in some cases a straightforward distinction between magmatic and metamorphic zircon (e.g., Harley and Black, 1997; Corfu et al., 2003; Kelly and Harley, 2005). Furthermore, experimental data are scarce and technically challenging (e.g., Ayers et al., 2003), limiting our interpretation of growth ages. This is particularly true when high pressure and high temperature conditions are explored, or when we are dealing with suspected polymetamorphic terranes. Metamorphic growth of zircon may occur not only during the thermal peak, but also along the prograde and retrograde path (Roberts and Finger, 1997; Liati and Gebauer, 1999; Vavra et al., 1999; Hermann et al., 2001). Moreover, it is commonly accepted that Th/U ratios lower than 0.1 indicate zircon growth under metamorphic conditions, whereas higher ratios are found in magmatic environments (Williams et al., 1997).

However, some of these one-to-one correspondences have been defied in a few cases; whether it be metamorphic zircon with high Th/U ratios (see Harley et al., 2007 and references therein) or the unconventional correspondence between oscillatory zoning and an eclogitic origin for zircon (Gebauer et al., 1997; Rubatto et al., 1998; Bingen et al., 2001; Corfu et al., 2002; cited by Corfu et al., 2003). In such cases, the problem is solved falling back on previous geochronological studies to interpret the obtained age, but the distinctive composition of zircon grown under eclogitic conditions can be used as well to determine its origin (e.g. Young and Kylander-Clark, 2015; Paquette et al., 2017; Lotout et al., 2018).

In this paper, we present one of these examples where both the zircon texture and the Th/U ratio strongly suggest that the obtained age could be interpreted as igneous; whereas, in addition to regional evidence, the REE composition of zircon provides a more complete way to link ages to geological processes.

2 Geological Setting

The Cabo Ortegal Complex is one of the allochthonous complexes cropping out in NW Iberia. These complexes record the protracted history of the northern margin of Gondwana from Cambrian-Ordovician times to the Variscan orogeny (Martínez Catalán et al., 2009, 2019). A recent paper explores the connection between

https://doi.org/10.5194/se-2020-53
Preprint. Discussion started: 14 May 2020
© Author(s) 2020. CC BY 4.0 License.

Solid Earth
Discussions
Open Access
EGU

the Iberian allochthonous complexes and some units present in the Armorican Massif (Ballèvre et al., 2014), grouping all of them into lower, middle and upper allochthon depending on their tectonometamorphic evolution and structural position. In NW Iberia, the lower allochthon is a Lower Cambrian siliciclastic sequence, intruded by a Lower Ordovician bimodal magmatism, which experienced high pressure and low to intermediate temperature metamorphism during the Middle Devonian (Díez Fernández et al., 2012a, 2012b; Abati et al., 2010; López Carmona et al., 2013). It represents the most external margin of Gondwana. The middle allochthon is mainly composed of mafic and ultramafic rocks interpreted as fragments of oceanic lithosphere; the oldest (~495 Ma) is related to the Iapetus-Tornquist Ocean, whereas the youngest (~395 Ma) is probably related to the Rheic Ocean (see Arenas et al., 2014, Martínez Catalán et al., 2019 and references therein). The upper allochthon is interpreted as a volcanic arc, and it can be divided according to their metamorphic evolution into HP-HT units, bellow, and intermediate-P units, above. In the Cabo Ortegal Complex, the HP-HT units define an overturned thinned sequence of rocks that is composed, from bottom to top, of quartzo-feldspathic gneisses, eclogites, mafic granulites and ultramafic peridotites (Fig. 1). Regarding the age of this HP-HT event, a first group of authors have proposed a single event occurring during the Devonian (~390 Ma, e.g., Ordóñez Casado et al., 2001) based on geochronology of eclogites and granulites. In contrast, a second group of authors have found evidences for a previous HP-HT metamorphic event at Cambro-Ordovician times, whereas the younger metamorphic event could have been HT, but definitely not HP (Fernández Suárez et al., 2002). A general HP/UHP-HT event occurring not before 390-400 Ma has been proposed by Arenas et al. (2014), taking into account regional data from different allochthonous complexes in NW Iberia and France. Those ages imply Early-Middle Devonian subduction of the HP-HT allochthonous units and eventually an accretionary process probably to Laurussia (Ballèvre et al., 2014; Martínez Catalán et al., 2019). This event would be interpreted as the first collisional evidence of the Variscan orogeny in Europe.

3 Sample preparation and zircon description

The eclogite studied in this work is a block-in-matrix included in quartzo-feldspathic gneisses located in the Cariño beach (sample COZ-4, lab number 110405, Fig. 1). The gneisses correspond to the Banded Gneisses Formation defined by Vogel (1967), mainly constituted by migmatitic garnet- and kyanite-bearing quartzo-feldspathic gneisses with inclusions of eclogite, mafic granulites and calc-silicate rocks (Vogel, 1967; Gil Ibarguchi et al., 1990; Fernández, 1997). Lithological and mineralogical composition is heterogeneous and thickness variable (> 200 m), with gradational contacts between layers locally enriched in garnet or amphibole. Intercalations of leucocratic garnet-bearing orthogneisses, coronitic metagabbros and dioritic dykes evidence also an old magmatism.

The sample COZ-4 has a granoblastic texture and it is mainly composed of omphacite and garnet with honeycomb texture. Biotite, brown amphibole, calcite, sulphides and rutile appear as minor phases. The eclogite block has an ellipsoid shape of ratio 1:1:2. The section YZ of the ellipsoid is a square of approximately of 1 m^2 with sharp limits and rounded corners. It is enclosed in a phyllonite matrix formed basically by serpentinite and amphibole. The matrix is well-foliated obliquely to the main foliation, whereas the eclogite block is not foliated and has granoblastic texture. Oblique foliation is disposed parallel to the foliation planes of refolded decimeter-scale folds and sheath folds with top-to-the-N20E sense of movement. The structural relationships between the

https://doi.org/10.5194/se-2020-53
Preprint. Discussion started: 14 May 2020
© Author(s) 2020. CC BY 4.0 License.


eclogite block and the banded gneisses evidence a high competence contrast, where the block is passively displaced during all the deformation process.

Metamorphic evolution of the enclosing eclogitic banded gneisses recorded a HP-HT event followed by a fast exhumation under granulite and finally amphibolite facies metamorphism, with extensive partial melting. The eclogite P-T conditions calculated from omphacite-garnet-bearing mafic rock indicated 22 kbar and 780-800 ºC (Basterra et al., 1989; Gil Ibarguchi et al., 1990; Mendia, 2000; Albert et al., 2012).

Mineral separation was carried out at the Universidad Complutense (Madrid) and it involved an initial concentration of heavy minerals using a Wilfley table, the sieving of the resulting sample below 0.2 mm, the separation of the magnetic minerals with a Franz isodynamic magnetic separator, and the final concentration with methylene iodide (MEI). A significant amount of heavy minerals was obtained, mainly rutile and sulphides, whereas the zircon yield was poor (hardly 50 grains out of 30 kg of sample). Zircon grains are usually fragments, typical of populations extracted from mafic rocks (Corfu et al., 2003), varying in size from 0.1 to 0.2 mm across. Still, in a few grains it is possible to recognize some crystal faces. Zircon is colorless with scarce mineral or fluid inclusions.

The zircon grains were mounted on glass slides with a double-sided adhesive in parallel rows together with some grains of zircon standard R33 (Black et al., 2004) and set in epoxy resin. After the resin was cured, the mounts were ground down to expose their central portions. Prior to isotopic analysis, zircons were imaged with transmitted and reflected light on a petrographic microscope, and with cathodoluminescence (CL) on a JEOL 5600LV scanning electron microscope, housed at the Stanford-US Geological Survey microanalysis center (SUMAC). Following the analysis, secondary electron images were taken to determine the location of the spots.

Cathodoluminescence images of zircon grains from sample COZ-4 display a variety of textures (Fig. 2). The most common CL texture is a combination of oscillatory and sector zoning (grains #5, 6, 11, 13, 14, and 15, Fig. 2). Some zircon grains only have a well-defined oscillatory zoning with moderate to poor luminescence (grains #2, 8 and 9, Fig. 2), whereas other zircon grains exclusively show sector and fir-tree zoning with moderate luminescence (grains #1, 4, 7, 10 and 16, Fig. 2). Grain #2 also displays a non-luminescent homogeneous rim. There is a luminescent subrounded core (grain #3), which shows textures typically attributed to metamorphism, such as recrystallization and microveining, and it is mantled by zircon with a faint soccer-ball zoning, similar to grain #12. Grain #17 shows an irregular domainal texture (comparable to Fig. 3.5 in Corfu et al., 2003), interpreted as a result of strain during zircon growth. This internal patchy area is partially surrounded by new zircon not affected by strain and it presents broad and faint oscillatory zones.

In summary, following the most accepted interpretation of zircon textures (Corfu et al., 2003), most of the grains exhibit zoning typical of zircon grown in an igneous environment, except grains #3, #12, #17 and the rim in #2, which textures can be unequivocally interpreted as generated under metamorphic conditions.

4 Results

4.1 U-Pb SHRIMP-RG analyses

https://doi.org/10.5194/se-2020-53
Preprint. Discussion started: 14 May 2020
© Author(s) 2020. CC BY 4.0 License.

Zircon U-Th-Pb analyses were conducted on the sensitive high-resolution ion microprobe-reverse geometry (SHRIMP-RG) operated by the SUMAC facility (Stanford-USGS micro analysis center) at the Stanford University. An O^{2-} primary ion beam varying from 4 to 6 nA generates secondary ions from the target spot with a diameter of ~20 µm and a depth of 1-2 µm. As we assumed a Paleozoic age, the counting time for ^{206}Pb is increased to improve counting statistics and precision of the $^{206}Pb/^{238}U$ age. Concentration data were normalized against zircon standard CZ3 (550 ppm U, Pidgeon et al., 1994), and isotope ratios were calibrated against R33 (419 Ma, Black et al., 2004). Data reduction followed the methods described by Williams (1997), Ireland and Williams (2003), and Squid 1.08 and Isoplot 3.0 software (Ludwig, 2001, 2003) were used. The U-Pb zircon data are shown in Table DR-1.

Twenty analyses were performed in 17 zircon grains. The youngest result has high common Pb content and it will not be further considered in the discussion of the age (analysis #3.2). The following youngest result is obtained from a non-luminescent rim in grain #2 (369 Ma) and the seventeen remaining analyses are evenly distributed between 382 and 403 Ma (Fig. 3). The weighted mean obtained from eight analyses is 390.4±1.2 Ma, with a mean square of weighted deviation (MSWD) of 0.65. Finally, one analysis taken in a core yields the oldest age (474 Ma) and, in spite of its high common lead, its significance will be discussed later.

4.2 Trace element SHRIMP-RG analyses

After the isotopic analysis, the zircon mounts were lightly polished to remove the original gold coating and sputtered pits, and recoated with gold. Methods follow those presented by Mazdab (2009). A small spot diameter (about 15 µm) and a less energetic O^{-2} beam (between 1 and 2 nA) permitted that the analyses were conducted in a volume adjacent to that analyzed for isotopic compositions. The primary standard MAD is a gem quality crystal from Madagascar that has been extensively characterized in-house and found to be very chemically homogeneous (Mazdab and Wooden, 2006). The secondary zircon standard is CZ3 (see previous section). These standards were analyzed every ten unknowns over multiple analytical sessions to establish precision of the trace element analyses. The procedure to obtain concentrations from raw counts is described in Schwartz et al. (2010). Precision for Y at 2σ is ±6%; for the measured rare earth elements (REE, excluding La), Hf, Th, and U, 2σ precision ranges from ±8 to 18%; the precision for La is ±30%.

Even though we performed thirty-six trace element (TE) analyses in 19 zircon grains, in this work we are only reporting those analyses adjacent to a U-Pb spot (Table DR-2).

Uranium concentrations range from 55 to 1,150 ppm, most of the values are below 230 ppm and a group of five analyses aimed to the less luminescent areas yield values higher than 370 ppm. Thorium concentrations are generally low, scattered between 10 and 55 ppm, excepting the analyses in the less luminescent zones, which vary between 90 and 290 ppm. In the Th-U graph (Fig. 4a), the data show a good positive correlation and, with the exception of analysis #8.1, Th/U ratios are higher than 0.1.

Total REE concentrations are low and range from 30 to 350 ppm. In a chondrite-normalized REE diagram (Fig. 4b), all analyses depict similar patterns that are characterized by a moderate fractionation from lanthanum (La) to lutetium (Lu), with a prominent positive anomaly in cerium (Ce), absence of europium (Eu)

https://doi.org/10.5194/se-2020-53
Preprint. Discussion started: 14 May 2020
© Author(s) 2020. CC BY 4.0 License.


anomaly and a slightly negative slope in heavy (H) REE. The lack of a Eu anomaly is typically explained as the result of absence of plagioclase (Rubatto, 2002), whereas the high distribution coefficient for the HREE in garnet accounts for the remarkably depleted content in these elements and the resulting humped patterns in zircon (Kelly and Harley, 2005, and references therein). The combination of plagioclase absence and garnet presence is commonly attributed to eclogitic metamorphism (Puga et al., 2005; McClelland et al., 2006; Chen et al., 2010).

5 Interpretation and discussion

5.1 Interpretation of the results

Even though CL images are fundamental to select the best spots for analysis in complex zircon grains, it is clear that the evaluation of the geochronological results based only in the CL textures is not straightforward. In the zircon grains reported in this study, both CL textures and Th/U ratios strongly suggest that the obtained Middle Devonian age should correspond to the igneous protolith. However, this interpretation is inconsistent with previous geochronology studies and with the regional geology. On one hand, the age of other mafic and felsic rocks in the allochthonous complexes in NW Iberia varies between 520 and 470 Ma and there is no evidence of a Devonian magmatic event so far (e.g., Ordóñez Casado et al., 2001; Abati et al., 2007; Fernández Suárez et al., 2007; Andonaegui et al., 2012). On the other hand, several studies have suggested that there is a high-pressure–high-temperature metamorphic event in this unit during the Middle Devonian (Ordóñez Casado et al., 2001; Fernández Suárez et al., 2007).

The fallibility of the CL-Th/U–based geochronology can be easily circumvented in this case studying the REE composition of zircon. Under eclogitic conditions, this mineral exhibits a couple of diagnostic features such as depletion in HREE and absence of an Eu negative anomaly.

5.2 Origin of zircon

There are three main ways to form zircon in metamorphic environments (e.g., Young and Kylander-Clark, 2015): dissolution of existing grains and subsequent precipitation, recrystallization of former crystals, and new growth, either by Zr-releasing reactions or by direct crystallization from a partial melt or a fluid.

Dissolution and precipitation can be used to explain the texture and isotopic data from the only grain with a core-rim feature (grain #3 Fig. 2, Table DR-1). In spite of its high common Pb content, the age obtained in the core (~474 Ma) is equivalent to other ages found in the literature for the eclogitic protoliths (Bernard Griffiths et al., 1985; Peucat et al., 1990; Ordoñez Casado et al., 2001), whereas the rim age (~360 Ma) is probably affected by lead loss. In any case, the absence of xenocrystic cores in the rest of the grains suggests that dissolution and precipitation was subordinate and other zircon-forming processes were active in this eclogite.

https://doi.org/10.5194/se-2020-53
Preprint. Discussion started: 14 May 2020
© Author(s) 2020. CC BY 4.0 License.

Solid Earth
Discussions
Open Access
EGU

Even though zircon recrystallization during metamorphism usually disturbs the former igneous zoning, Schaltegger et al. (1999) report a U-loss process during zircon recrystallization that results in a weakening of CL intensity, without losing the oscillatory zoning. However, this annealing is usually coupled with partial U-Pb resetting. In our case, data are tightly grouped and they are equivalent to other ages obtained for the HP-HT metamorphism in adjacent areas (e.g., Ordoñez Casado et al., 2001), making this argument unsound.

Other possibility is that new zircon grew during eclogite metamorphism. Direct crystallization from a melt or a fluid has been invoked in the few studies where oscillatory zoning was found in eclogitic zircon (Gebauer et al., 1997; Rubatto et al., 1998). However, crystallization from a fluid can be discarded as zircons grown that way usually have Th/U ratios lower than 0.1 (Rubatto et al., 1998). On the other hand, zircon crystallization from a melt generated during eclogitic metamorphism could show Th/U ratios higher than 0.1. In that case, the system would be open, making HREE available for both garnet and zircon (Rubatto, 2002). Nevertheless, the REE pattern of the zircon analyzed precludes this possibility. Alternatively, zircons could be generated from metamorphic reaction in solid state. The abundance of rutile suggests that titanite or ilmenite were also present in the protolith, making any of these two minerals the ideal precursors for zircon (Bingen et al., 2001; Bea et al., 2006).

5.3 Implications for the geochronology of the upper allochthon

The assortment of geochronological results in the upper allochthon (Fig. 5) could be indicating that the rocks grouped under this denomination have different origins, even though they are considered as different crustal sections of a volcanic arc. This is coherent with the heterogeneity of the allochthonous sequences at different scales, including significant differences in the structural and metamorphic evolution (e.g., Castiñeiras, 2005; Gómez Barreiro et al., 2006, 2007; Paquette et al., 2017). The good correlation of Lower, Middle and Upper allochthon across the allochthonous complexes of NW Iberia and France support the general tectonic setting but does not exclude the possibility that several lithospheric fragments were amalgamated under similar conditions during the activity of the system. In addition, it should be noted that the variety of techniques and the interpretation of age data does not show the same degree of robustness and could also contribute to the apparent dispersion of ages (see Paquette et al., 2017, Lotout et al., 2018).

The combination of the trace elements (TE) signature, CL images and a high-resolution ion probe emerges as an excellent approach to overcome regional uncertainty in the studied case as previously stated in similar context (e.g. Lotout et al., 2018). The positive correlation of TE evolution and metamorphic assemblage let us connect textural information and regional evidence with geochronology, which was not considered in previous works.

Due to the correlation between metamorphic evolution and TE data, we suggest that the analyzed zircons represent part of the eclogite facies assemblage, so that a HP event about 390 Ma is favored. It should be noted that the existence of a previous (pre-400 Ma) HP event is not dismissed but specific experiments need to be conducted to figure out its geological meaning (e.g. Lotout et al 2018).

https://doi.org/10.5194/se-2020-53
Preprint. Discussion started: 14 May 2020
© Author(s) 2020. CC BY 4.0 License.

Solid Earth
Discussions
Open Access
EGU

248 **5.4 concluding remarks**

249 We have dated zircons from an eclogitic block-in-matrix with a combination of high-resolution ion probe, CL-
250 image and TE data. Strengths and weakness of those techniques have been discussed and correlated with
251 regional knowledge. An age about 390 Ma has been identified and linked to an eclogite facies mineral
252 assemblage based on zircon TE data. These data represent the most robust evidence of an eclogite facies event
253 at 390 Ma for the allochthonous complexes of the NW Iberia.
254 Our results indicate that well-known techniques (CL) and geochemical relationships (Th/U) must be used in
255 combination with TE data and structural relationships as provenance/process gauges, particularly in complex
256 orogenic scenarios or extreme environments. While geochronology provides accurate isotope relationships, their
257 temporal dimension must rely on structural and petrological evidence.
258
259 *Data availability*
260 The data are not publicly accessible
261
262 *Supplement*
263 Tables DR-1, with U-Pb isotopic zircon data, and DR-2, with REE zircon composition, is available online
264 at___[link to be included by Solid Earth]_____
265
266 *Author contributions*
267 PC, JGB contributed equally to the field, experimental and elaboration of the manuscript. CA and JMBP
268 contribute to U-Pb data acquisition, processing and interpretation, and FJF participated in the fieldwork and the
269 geological interpretation.
270
271 *Competing interests*
272 The authors declare that they have no conflict of interest.

273 **Acknowledgements**

274 Carmen Valdehita is thanked for her assistance during mineral separation. Fieldwork, sample separation and
275 analytical expenses were financed by Universidad Complutense (Madrid) through the Grupo de Investigación
276 UCM Eurovarisco (910129). PC and JGB benefited from two travel aids of the “Programa de ayudas a
277 investigadores del CSIC para la realización de estancias en centros de investigación extranjeros”. CA travel was
278 financed by projects CGL-2007-66857CO2-02 and CGL2010-21298 of the Spanish Commission for Science
279 and Technology. JGB acknowledges financial support from the Ramón y Cajal Program (RYC-2010-05818).
280 Funds from the Projects CGL2010-14890 and CGL2011-23628/BTE of the Spanish Secretary of State for
281 Research, Development and Innovation and projects CGL2011-22728 and CGL2016-78560-P of the Spanish
282 Ministry of Economy, Industry and Competitiveness, as part of the National Program of Projects in
283 Fundamental Research are kindly acknowledged. JMBP appreciates financial support by the Spanish Ministry
284 of Economy, Industry and Competitiveness though the Formación de Profesional Investigador grant FPI 2013-

https://doi.org/10.5194/se-2020-53
Preprint. Discussion started: 14 May 2020
© Author(s) 2020. CC BY 4.0 License.


2016 (BES-2012-059893). JGB appreciates financial support by the Spanish Ministry of Science and Innovation through the IEDI-2016-00691 fellowship.

References

Abati, J., Castiñeiras, P., Arenas, R., Fernández Suárez, J., Gómez-Barreiro, J., and Wooden, J., 2007, Using SHRIMP zircon dating to unravel tectonothermal events in arc environments. The early Palaeozoic arc of NW Iberia revisited, Terra Nova, 19, 432–439. https://doi.org/10.1111/j.1365-3121.2007.00768.x

Abati, J., Dunning, G.R., Arenas, R., Díaz García, F., González Cuadra, P., Martínez Catalán, .J.R., and Andonaegui, P., 1999, Early Ordovician orogenic event in Galicia (NW Spain): evidence from U-Pb ages in the uppermost unit of the Ordenes Complex, Earth Planet. Sci. Lett., 165, 213–228. https://doi.org/10.1016/S0012-821X(98)00268-4

Abati, J., Gerdes, A., Fernández-Suárez, J., Arenas, R., Whitehouse, M.J., and Díez-Fernández, R., 2010, Magmatism and early-Variscan continental subduction in the northern Gondwana margin recorded in zircons from the basal units of Galicia, NW Spain, Geol. Soc. Am. Bull., 122, 219–235. doi: 10.1130/B26572.1.

Albert, R., Arenas, R., Sánchez Martínez, S., and Gerdes, A., 2012, The eclogite facies gneisses of the Cabo Ortegal Complex (NW Iberian Massif): Tectonothermal evolution and exhumation model, J. Iberian Geol., 38, 389–406, doi: 10.5209/rev_JIGE.2012.v38.n2.40465.

Anders, E., and Grevesse, N., 1989, Abundances of the elements: Meteoritic and solar, Geochimica et Cosmochimica Acta, 53, 197–214. https://doi.org/10.1016/0016-7037(89)90286-X

Andonaegui, P., Castiñeiras, P., González Cuadra, P., Arenas, R., Sánchez Martínez, S., Abati, J., Díaz García, F., and Martínez Catalán, J.R., 2012, The Corredoiras orthogneiss (NW Iberian Massif): Geochemistry and geochronology of the Paleozoic magmatic suite developed in a peri-Gondwanan arc, Lithos, 128-131, 84–99, doi: 10.1016/j.lithos.2011.11.005.

Arenas, R., Fernández, R.D., Martínez, S.S., Gerdes, A., Fernández-Suárez, J., Albert, R. 2014, Two-stage collision: Exploring the birth of Pangea in the Variscan terranes, Gondwana Research, 25, 756–763, doi: 10.1016/j.gr.2013.08.009.

Ayers, J.C., DeLaCruz, K., Miller, C., and Switzer, O., 2003, Experimental study of zircon coarsening in quartzite ±H2O at 1.0 GPa and 1000 ºC, with implications for geochronological studies of high-grade metamorphism, American Mineralogist, 88, 365–376. https://doi.org/10.2138/am-2003-2-313.

Ballèvre, M., Martínez Catalán, J.R., López-Carmona, A., Abati, J., Díez Fernández, R., Ducassou, C., Pitra, P., Arenas, R., Bosse, V., Castiñeiras, P., Fernández-Suárez, J., Gómez Barreiro, J., Paquette, J.L., Peucat, J.J., Poujol, M., Ruffet, G., and Sánchez Martínez, S., 2014, Correlation of the

https://doi.org/10.5194/se-2020-53
Preprint. Discussion started: 14 May 2020
© Author(s) 2020. CC BY 4.0 License.


320 nappe stack in the Ibero-Armorican arc across the Bay of Biscay: a joint French-Spanish project, in
321 Schulmann, K., Oggiano, G., Lardeaux, J.M., Janousek, V., Martínez Catalán, J.R., Scrivener, R.,
322 eds., The variscan orogeny: extent, timescale and the formation of the European Crust: London,
323 Geological Society, London, Special Publications, 405, 77-113, https://doi.org/10.1144/SP405.13.

324 Basterra, R., Cassi, J.M., Pérez San Román, L., Tascon, A., and Gil Ibarguchi, J.I., 1989, Evolución
325 metamórfica de las rocas pelíticas y semipelíticas de las formaciones Banded Gneises y Gneises de
326 Cariño (Cabo Ortegal, NW España), Studia Geologica Salmanticensia, 4, 133–146.

327 Bea, F., Montero, P., and Ortega, M., 2006, A LA-ICPMS evaluation of Zr reservoirs in common
328 crustal rocks: Implications for zircon-forming processes, Canadian Mineralogist, 44, 745–766.
329 https://doi.org/10.2113/gscanmin.44.3.693

330 Berger, J., Féménias, O., Ohnenstetter, D., Bruguier, O., Plissart, G., Mercier, J.C.C., and Demaiffe,
331 D., 2010, New occurrence of UHP eclogites in Limousin (French Massif Central): Age, tectonic
332 setting and fluid–rock interactions, Lithos, 118, 365–382, doi:10.1016/j.lithos.2010.05.013.

333 Bernard-Griffiths, J., Peucat, J.J., Cornichet, J., Iglesias Ponce de León, M., and Gil Ibarguchi, J.I.,
334 1985, U-Pb, Nd isotope and REE geochemistry in eclogites from the Cabo Ortegal Complex, Galicia,
335 Spain: an example of REE immobility conserving MORB-like patterns during high-grade
336 metamorphism, Chem. Geol., 52, 217–225. https://doi.org/10.1016/0168-9622(85)90019-3.

337 Bingen, B., Davis, W.J., and Austrheim, H., 2001, Zircon U-Pb geochronology in the Bergen arc
338 eclogites and their Proterozoic protoliths, and implications for the pre-Scandian evolution of the
339 Caledonides in western Norway, Geological Society of America Bulletin, 113, 640–649.
340 https://doi.org/10.1130/0016-7606(2001)113<0640:ZUPGIT>2.0.CO;2

341 Black, L.P., Kamo, S.L., Allen, C.M., Davis, D.W., Aleinikoff, J.N., Valley, J.W., Mundil, R.,
342 Campbell, I.H., Korsch, R.J., Williams, I.S., and Foudoulis, C., 2004, Improved 206Pb/238U
343 microprobe geochronology by the monitoring of a trace-element-related matrix effect, SHRIMP, ID-
344 TIMS, ELA-ICP-MS and oxygen isotope documentation for a series of zircon standards, Chemical
345 Geology, 205, 115–140. https://doi.org/10.1016/j.chemgeo.2004.01.003.

346 Castiñeiras, P., 2005, Origen y evolución tectonotermal de las Unidades de O Pino y Cariño
347 (Complejos Alóctonos de Galicia): A Coruña, Nova Terra 28, 279 p.

348 Castiñeiras, P., Díaz García, F., and Gómez Barreiro, J., 2010, REE-assisted U-Pb zircon age
349 (SHRIMP) of an anatectic granodiorite: constraints on the evolution of the A Silva granodiorite,
350 Iberian Allochthonous Complexes, Lithos, 116, 153–166, doi: 10.1016/j.lithos.2010.01.013.

351 Chen Ren Xu, Zheng Yong-Fei, and Xie, Liewen, 2010, Metamorphic growth and recrystallization of
352 zircon: Distinction by simultaneous in-situ analyses of trace elements, U-Th-Pb and Lu-Hf isotopes in

https://doi.org/10.5194/se-2020-53
Preprint. Discussion started: 14 May 2020
© Author(s) 2020. CC BY 4.0 License.


zircons from eclogite-facies rocks in the Sulu orogen, Lithos, 114, 132–154. https://doi.org/10.1016/j.lithos.2009.08.006.

Corfu, F., Hanchar, J.M., Hoskin, P.W.O., and Kinny, P., 2003, Atlas of zircon textures, in Hanchar, J.M., and Hoskin, P.W.O., eds., Zircon: Washington, Mineralogical Society of America, Reviews in Mineralogy and Geochemistry 53, 468–500. https://doi.org/10.2113/0530469.

Corfu, F., Krogh Ravna, E., and Kullerud, K., 2002, A Late Ordovician U-Pb age for HP metamorphism of the Tromsdalstind eclogite of the Uppermost Allochthon of the Scandinavian Caledonides: Davos, Switzerland, 12th Goldschmidt Conference, p. 18–23.

Dallmeyer, R.D., and Tucker, R.D., 1993, U-Pb zircon age for the Lagoa augen gneiss, Morais Complex, Portugal: tectonic implications, Journal of the Geological Society, London, 150, 405–410. https://doi.org/10.1144/gsjgs.150.2.0405

Dallmeyer, R.D., Martínez Catalán, J.R., Arenas, R., Gil Ibarguchi, J.I., Gutiérrez Alonso, G., Farias, P., Aller, J., and Bastida, F., 1997, Diachronous Variscan tectonothermal activity in the NW Iberian Massif: Evidence from $^{40}Ar/^{39}Ar$ dating of regional fabrics, Tectonophysics, 277, 307–337. https://doi.org/10.1016/S0040-1951(97)00035-8.

Díez Fernandez, R., Castiñeiras, P., and Gómez Barreiro, J., 2012a, Age constraints on Lower Paleozoic convection system: magmatic events in the NW Iberian Gondwana margin, Gondwana Research, 21, 1066–1079. https://doi.org/10.1016/j.gr.2011.07.028.

Díez Fernández, R., Martínez Catalán, J.R., Arenas, R., Abati, J., Gerdes, A., and Fernández Suárez, J., 2012b, U-Pb detrital zircon analysis of the lower allochthon of NW Iberia: age constraints, provenance and links with the Variscan mobile belt and Gondwanan cratons, Journal of the Geological Society of London, 169, 655–665. https://doi.org/10.1144/jgs2011-146.

Fernández, F.J., 1997. Estructuras desarrolladas en gneises bajo condiciones de alta P y T (Gneises de Chímparra, Cabo Ortegal): A Coruña, Nova Terra 13, p. 250.

Fernández-Suárez, J., Arenas, R., Abati, J., Martínez Catalán, J.R., Whitehouse, M.J., and Jeffries, T.E., 2007, U-Pb chronometry of polymetamorphic high-pressure granulites: An example from the allochthonous terranes of the NW Iberian Variscan belt, *in* Hatcher, R.D., Jr., Carlson, M.P., McBride, J.H., and Martínez Catalán, J.R., eds., 4-D Framework of Continental Crust: Boulder, Colorado, Geological Society of America Memoir 200, p. 469–488, doi: 10.1130/2007.1200(24).

Fernández-Suárez, J., Corfu, F., Arenas, R., Marcos, A., Martínez Catalán, J., García, F., Abati, J., and Fernández, F.J., 2002, U-Pb evidence for a polyorogenic evolution of the HP-HT units of the NW Iberian Massif, Contributions to Mineralogy and Petrology, 143, 236–253. https://doi.org/10.1007/s00410-001-0337-2.

https://doi.org/10.5194/se-2020-53
Preprint. Discussion started: 14 May 2020
© Author(s) 2020. CC BY 4.0 License.


387 Gebauer, D., Schertl, H., Brix, M., and Schreyer, W., 1997, 35 Ma old ultrahigh-pressure
388 metamorphism and evidence for very rapid exhumation in the Dora Maira Massif, Western Alps,
389 Lithos, 41, 5–24. https://doi.org/10.1016/S0024-4937(97)82002-6.

390 Gil Ibarguchi, J.I., Mendia, M., Girardeau, J., and Peucat, J.J, 1990, Petrology of eclogites and
391 clinopyroxene-garnet metabasites from the Cabo Ortegal Complex (northwestern Spain), Lithos, 25,
392 133–162, https://doi.org/10.1016/0024-4937(90)90011-O.
393 Gómez Barreiro, J., Martínez Catalán, J.R., Arenas, R., Castiñeiras, P., Abati, J., Díaz García, F., and
394 Wijbrans, J.R., 2007, Tectonic evolution of the upper allochthon of the Órdenes Complex
395 (northwestern IberianMassif): structural constraints to a polyorogenic peri-Gondwanan terrane, *in*
396 Linnemann, U., Nance, R.D., Kraft, P., and Zulauf, G., eds., The evolution of the Rheic Ocean: from
397 Avalonian–Cadomian active margin to Alleghenian–Variscan collision: Boulder, Colorado,
398 Geological Society of America Special Paper 423, 315–332. https://doi.org/10.1130/2007.2423(15).
399 Gómez Barreiro, J., Wijbrans, J.R., Castiñeiras, P., Martínez Catalán, J.R., Arenas,R., Díaz García, F.,
400 and Abati, J., 2006, 40Ar/39Ar laser probe dating of mylonitic fabrics in polyorogenic terrane of NW
401 Iberia, Journal of the Geological Society of London, 163, 61–73. https://doi.org/10.1144/0016-
402 764905-012
403 Harley S.L., and Black L.P., 1997, A revised Archaean chronology for the Napier Complex, Enderby
404 Land, from SHRIMP ion-microprobe studies, Antarctic Science, 9, 74–91.
405 https://doi.org/10.1017/S0954102097000102.
406 Harley, S.L., Kelly, N.M., and Möller, A., 2007, Zircon behaviour and the thermal histories of
407 mountain chains, Elements, 3, 25–30. https://doi.org/10.2113/gselements.3.1.25
408 Hermann, J., Rubatto, D., Korsakov, A., and Shatsky, V., 2001, Multiple zircon growth during fast
409 exhumation of diamondiferous, deeply subducted continental crust (Kokchetav Massif, Kazakhstan),
410 Contributions to Mineralogy and Petrology, 141, 66–82. https://doi.org/10.1007/s004100000218
411 Ireland, T.R., and Williams, I.S., 2003, Considerations in zircon geochronology by SIMS, in Hanchar,
412 J.M., and Hoskin, P.W.O., eds., Zircon: Washington, Mineralogical Society of America, Reviews in
413 Mineralogy and Geochemistry, 53, 215–241. https://doi.org/10.2113/0530215
414 Kelly, N.M., and Harley, S.L., 2005, An integrated microtextural and chemical approach to zircon
415 geochronology: refining the Archean history of the Napier Complex, east Antarctica, Contributions to
416 Mineralogy and Petrology, 149, 57–84. https://doi.org/10.1007/s00410-004-0635-6.
417 Korotev, R.L. 1996, A self-consistent compilation of elemental concentration data for 93 geochemical
418 reference samples, Geostandards Newsletter, 20, 217–245. https://doi.org/10.1111/j.1751-
419 908X.1996.tb00185.x.
420 Kuijper, R.P., Priem, H.N.A., and Den Tex, E., 1982, Late Archaean-early proterozoic source ages of
421 zircons in rocks from the Paleozoic orogen of western Galicia, NW Spain, Precambrian Research, 19,
422 1–29, doi: 10.1016/0301-9268(82)90017-1.

https://doi.org/10.5194/se-2020-53
Preprint. Discussion started: 14 May 2020
© Author(s) 2020. CC BY 4.0 License.


423 Liati, A., and Gebauer, D., 1999, Constraining the prograde and retrograde P-T-t path of Eocene HP
424 rocks by SHRIMP dating of different zircon domains: inferred rates of heating, burial, cooling and
425 exhumation for central Rhodope, northern Greece, Contributions to Mineralogy and Petrology, 135,
426 340–354, https://doi.org/10.1007/s004100050516.
427 López Carmona, A., Pitra, P., and Abati, J., 2013, Blueschist-facies metapelites from the Malpica–Tui
428 Unit (NW Iberian Massif): phase equilibria modelling and H_2O and Fe_2O_3 influence in high-pressure
429 assemblages, Journal of Metamorphic Geology, 31, 263–280, https://doi.org/10.1111/jmg.12018.
430 Lotout, C., Pitra, P., Poujol, M., Anczkiewicz, R., and Van Den Driessche, J. (2018). Timing and
431 duration of Variscan high-pressure metamorphism in the French Massif Central: A multimethod
432 geochronological study from the Najac Massif. Lithos, 308, 381-394.
433 https://doi.org/10.1016/j.lithos.2018.03.022.
434 Ludwig, K.R., 2001, Squid, A users manual, Berkeley Geochronology Center Special Publication No.
435 2.
436 Ludwig, K.R., 2003, Isoplot 3.00, a geochronological toolkit for Excel, Berkeley Geochronology
437 Center Special Publication No. 4.
438 Martínez Catalán, J.R., Arenas, R., Abati, J., Sánchez Martínez, S., Díaz García, F., Fernández
439 Suárez, J., González Cuadra, P., Castiñeiras, P., Gómez Barreiro, J., Díez Montes, A., González
440 Clavijo, E., Rubio Pascual, F.J., Andonaegui, P., Jeffries, T.E., Alcock, J.E., Díez Fernández, R., and
441 López Carmona, A., 2009, A rootless suture and the loss of the roots of a mountain chain: The
442 Variscan belt of NW Iberia, Comptes Rendus Geoscience, 341, 114–126.
443 https://doi.org/10.1016/j.crte.2008.11.004.
444 Martínez Catalán, J.R., Gómez Barreiro, J., Dias da Silva, I., Chichorro, M., López-Carmona, A.,
445 Castiñeiras, P., Abati, J., Andonaegui, P., Fernández-Suárez, J., González Cuadra, P., Benítez-Pérez,
446 J. M. (2019): Variscan Suture Zone and Suspect Terranes in the NW Iberian Massif: Allochthonous
447 Complexes of the Galicia-Trás os Montes Zone (NW Iberia). In: Quesada, C. and Oliveira, T. (eds.):
448 *The Geology of Iberia: A Geodynamic Approach*, pp. 99-130. Springer, Cham.
449 https://doi.org/10.1007/978-3-030-10519-8_4.
450 Mateus, A., Munhá, J., Ribeiro, A., Tassinari, C. C. G., Sato, K., Pereira, E., and Santos, J. F. (2016).
451 U–Pb SHRIMP zircon dating of high-grade rocks from the Upper Allochthonous Terrane of Bragança
452 and Morais Massifs (NE Portugal); geodynamic consequences. Tectonophysics, 675, 23-49.
453 https://doi.org/10.1016/j.tecto.2016.02.048.
454 Mazdab, F.K., 2009, Characterization of flux-grown trace-element-doped titanite using the high-
455 mass-resolution ion microprobe (SHRIMP-RG), Canadian Mineralogist, 47, 813–831.
456 https://doi.org/10.3749/canmin.47.4.813.
457 Mazdab, F.K., and Wooden, J.L., 2006, Trace element analysis in zircon by ion microprobe
458 (SHRIMP-RG): technique and applications, Geochimica et Cosmochimica Acta Supplement, 70, 405,
459 10.1016/j.gca.2006.06.817.

https://doi.org/10.5194/se-2020-53
Preprint. Discussion started: 14 May 2020
© Author(s) 2020. CC BY 4.0 License.


460 McClelland, W.C., Power, S.E., Gilotti, J.A., Mazdab, F.K., and Wopenka, B., 2006, U-Pb SHRIMP
461 geochronology and trace-element geochemistry of coesite-bearing zircons, North-East Greenland
462 Caledonides, *in* Hacker, B.R., McClelland, W.C., and Liou, J.G., eds., Ultrahigh-pressure
463 metamorphism: Deep continental subduction: Boulder, Colorado. Geological Society of America
464 Special Paper 403, 23–43, https://doi.org/10.1130/2006.2403(02).
465 Mendia, M.S., 2000, Petrología de la Unidad Eclogítica del Complejo de Cabo Ortegal (NW de
466 España): A Coruña, Nova Terra 16, p. 424.
467 Ordoñez Casado, B., Gebauer, D., Schäfer, H.J., Ibarguchi, G., and Peucat, J.J., 2001, A single
468 Devonian subduction event for the HP/HT metamorphism of Cabo Ortegal complex within the Iberian
469 Massif, Tectonophysics, 3, 359–385, https://doi.org/10.1016/S0040-1951(00)00210-9.
470 Peucat, J.J., Bernard-Griffiths, J., Gil Ibarguchi, J.I., Dallmeyer, R.D., Menot, R.P., Cornichet, J., and
471 Iglesias Ponce de Leon, M., 1990, Geochemical and geochronological cross section of the deep
472 Variscan crust: The Cabo Ortegal high-pressure nappe (Northwestern Spain), Tectonophysics, 177,
473 263–292. https://doi.org/10.1016/0040-1951(90)90285-G.
474 Paquette, J. L., Ballèvre, M., Peucat, J. J., Cornen, G. (2017). From opening to subduction of an
475 oceanic domain constrained by LA-ICP-MS U-Pb zircon dating (Variscan belt, Southern Armorican
476 Massif, France). Lithos, 294, 418-437. https://doi.org/10.1016/j.lithos.2017.10.005.
477 Pidgeon R.T., Furfaro D., Kennedy A.K., Nemchin A.A., Van Bronswjk W., 1994, Calibration of
478 zircon standards for the Curtin SHRIMP II: Abstracts of the eighth International Conference on
479 Geochronology, Cosmochronology and Isotope Geology, U.S. Geological Survey Circular v. 1107, p.
480 251.
481 Puga, E., Fanning, C.M., Nieto, J.M., and Díaz de Federico A., 2005, Recrystallization textures in
482 zircon generated by ocean-floor and eclogite-facies metamorphism, a cathodoluminescence and U-Pb
483 SHRIMP study, with constraints from REE elements, Canadian Mineralogist, 43, 183–202.
484 https://doi.org/10.2113/gscanmin.43.1.183.
485
486 Roberts, M., and Finger, F., 1997, Do U-Pb zircon ages from granulites reflect peak metamorphic
487 conditions?, Geology, 25, 319–322. https://doi.org/10.1130/0091-
488 7613(1997)025<0319:DUPZAF>2.3.CO;2.
489 Rubatto, D., 2002, Zircon trace element geochemistry: partitioning with garnet and the link between
490 U–Pb ages and metamorphism, Chemical Geology, 184, 123–138. https://doi.org/10.1016/S0009-
491 2541(01)00355-2.
492 Rubatto, D., and Gebauer, D., 2000, Use of cathodoluminescence for U-Pb zircon dating by ion
493 microprobe: some examples from the Western Alps, *in* Pagel M., Barbin V., Blanc P., and
494 Ohnenstetter D., eds., Cathodoluminescence in geosciences: Berlin, Springer, 373–400.
495 https://doi.org/10.1007/978-3-662-04086-7_15.

https://doi.org/10.5194/se-2020-53
Preprint. Discussion started: 14 May 2020
© Author(s) 2020. CC BY 4.0 License.


496 Rubatto, D., Gebauer, D., and Fanning, M., 1998, Jurassic formation and Eocene subduction of the
497 Zermatt-Saas-Fee ophiolites: Implications for the geodynamic evolution of the Central and Western
498 Alps, Contributions to Mineralogy and Petrology, 132, 269–287,
499 https://doi.org/10.1007/s004100050421.
500 Santos Zalduegui, J.F., Schärer, U., Gil Ibarguchi, J.I., and Girardeau, J., 1996, Origin and evolution
501 of the Paleozoic Cabo Ortegal ultramafic-mafic complex (NW Spain): U-Pb, Rb-Sr and Pb-Pb isotope
502 data, Chemical Geology, 129, 281–304, https://doi.org/10.1016/0009-2541(95)00144-1.
503 Schaltegger U., Fanning C.M., Günther D., Maurin J.C., Schulmann K., and Gebauer D., 1999,
504 Growth, annealing and recrystallization of zircon and preservation of monazite in high-grade
505 metamorphism: conventional and in-situ U-Pb isotope, cathodoluminescence and microchemical
506 evidence, Contributions to Mineralogy and Petrology, 134, 186–201.
507 https://doi.org/10.1007/s004100050478.
508 Schwartz, J.J., John, B.E., Cheadle, M.J., Wooden, J.L., Mazdab, F., Swapp, S., and Grimes, C.B.,
509 2010, Dissolution-reprecipitation of igneous zircon in mid-ocean ridge gabbro, Atlantis Bank,
510 Southwest Indian Ridge, Chemical Geology, 274, 68–81.
511 https://doi.org/10.1016/j.chemgeo.2010.03.017.
512 Tomaschek, F., Kennedy, A., Villa, I., Lagos, M., and Ballhaus, C., 2003, Zircons from Syros,
513 Cyclades, Greece-Recrystallization and mobilization of zircon during high-pressure metamorphism,
514 Journal of Petrology, 44, 1977–2002. https://doi.org/10.1093/petrology/egg067.
515 Valverde Vaquero, P., and Fernández, F.J., 1996, Edad de enfriamiento U/Pb en rutilos del Gneis de
516 Chímparra (Cabo Ortegal, NO de España), Geogaceta, v. 20, p. 475–478.
517 van Calsteren, P.W.C., Boelrijk, N.A.I.M., Hebeda, E.H., Priem, H.N.A., Den Tex, E., Verdurmen,
518 E.A.T.H., and Verschure, R.H., 1979, Isotopic dating of older elements (including the Cabo Ortegal
519 mafic-ultramafic complex) in the Hercynian orogen of NW Spain: manifestations of a presumed Early
520 Paleozoic mantle plume, Chemical Geology, 24, 35–56. https://doi.org/10.1016/0009-2541(79)90011-
521 1.
522 Vavra, G., Schmid, R., and Gebauer, D., 1999, Internal morphology, habit and U-Th-Pb microanalysis
523 of amphibolite-to-granulite facies zircons: geochronology of the Ivrea Zone (Southern Alps),
524 Contributions to Mineralogy and Petrology, 134, 380–404. https://doi.org/10.1007/s004100050492.
525 Vogel, D.E., 1967, Petrology of an eclogite- and pirigarnite-bearing polymetamorphic rock complex
526 at Cabo Ortegal, NW Spain, Leidse Geologische Mededelingen, 40, 121–213.
527 Williams, I.S., 1997, U-Th-Pb geochronology by ion microprobe: not just ages but histories, Reviews
528 in Economic Geology, 7, 1–35. https://doi.org/10.5382/Rev.07.01.
529 Young, D.J. and Kylander-Clark, A.R.C., 2015, Does Continental Crust Transform during Eclogite-
530 Facies Metamorphism?, Journal of Metamorphic Geology, 33, 331-357.
531 https://doi.org/10.1111/jmg.12123.
532

https://doi.org/10.5194/se-2020-53
Preprint. Discussion started: 14 May 2020
© Author(s) 2020. CC BY 4.0 License.

533 **FIGURE CAPTIONS**

534 Figure 1. Geological map of the northern area of the Cabo Ortegal Complex with the location
535 of the sample.

536 Figure 2. Cathodoluminescence images of the analyzed zircons. Ellipses indicate the location
537 of the U-Pb spots, whereas circles represent the trace element analyses.

538 Figure 3. (A) Tera-Wasserburg diagram showing U-Pb data for the analyzed sample. Gray
539 ellipses represent data included in the calculated mean. (B) Age distribution of the data
540 considered in the mean age calculation.

541 Figure 4. (A) U versus Th and (B) chondrite-normalized REE patterns. Normalization values
542 after Anders and Grevesse (1989), modified by Korotev (1996).

543 Figure 5. Protolith and metamorphism ages in the upper allochthon, including the HP-HT and
544 the IP units. Abbreviations: Zrn, zircon; Mnz, monazite; Hbl, hornbende; Am, amphibole;
545 Ms, muscovite; Bt, biotite; Ttn, titanite; Ep, epidote; Rt, rutile; Phl, phlgopite; Ed, edenite;
546 WR, whole-rock; rcl, recalculated by Kuilper et al. (1982).

547

548 **Suplementary data**

549 Tables DR-1, with U-Pb isotopic zircon data, and DR-2, with REE zircon composition, is
550 available online at___[link to be included by Solid Earth]_____

https://doi.org/10.5194/se-2020-53
Preprint. Discussion started: 14 May 2020
© Author(s) 2020. CC BY 4.0 License.

Solid Earth
Discussions
Open Access
EGU

Figure 1

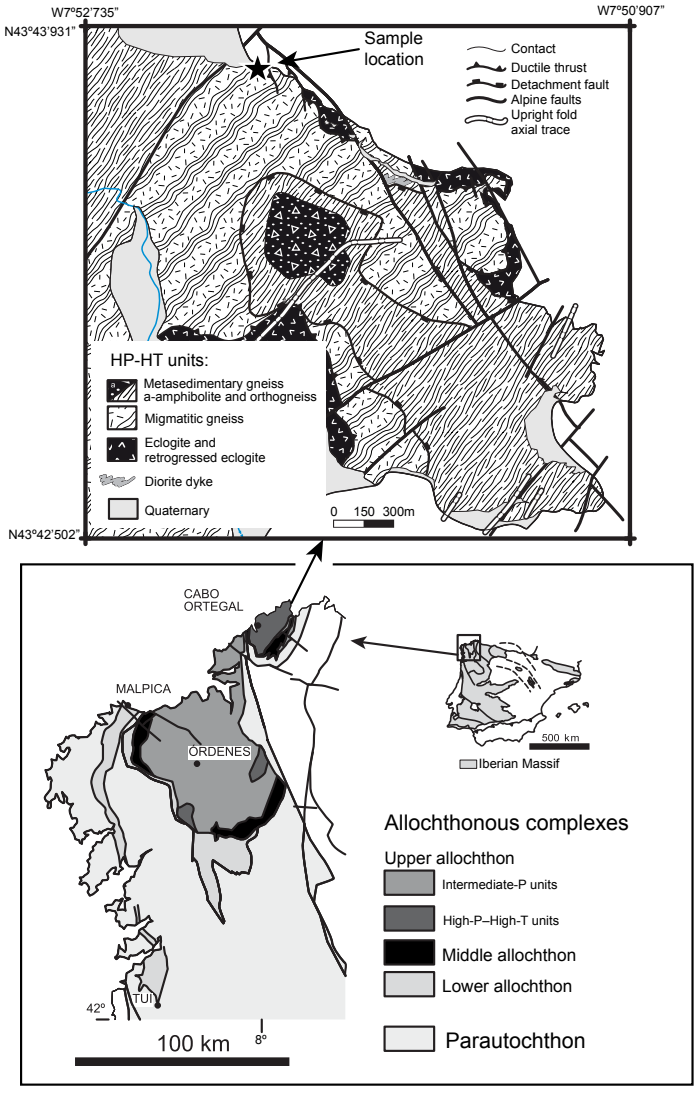

https://doi.org/10.5194/se-2020-53
Preprint. Discussion started: 14 May 2020
© Author(s) 2020. CC BY 4.0 License.

Solid Earth
Discussions
Open Access
EGU

Figure 2

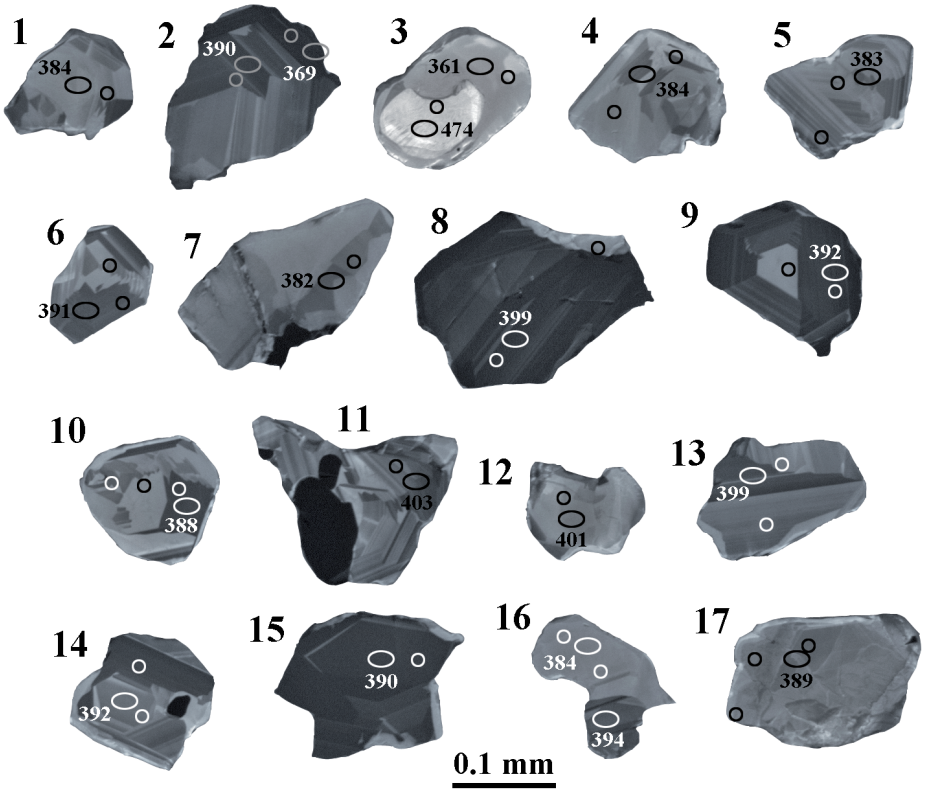

https://doi.org/10.5194/se-2020-53
Preprint. Discussion started: 14 May 2020
© Author(s) 2020. CC BY 4.0 License.

Figure 3

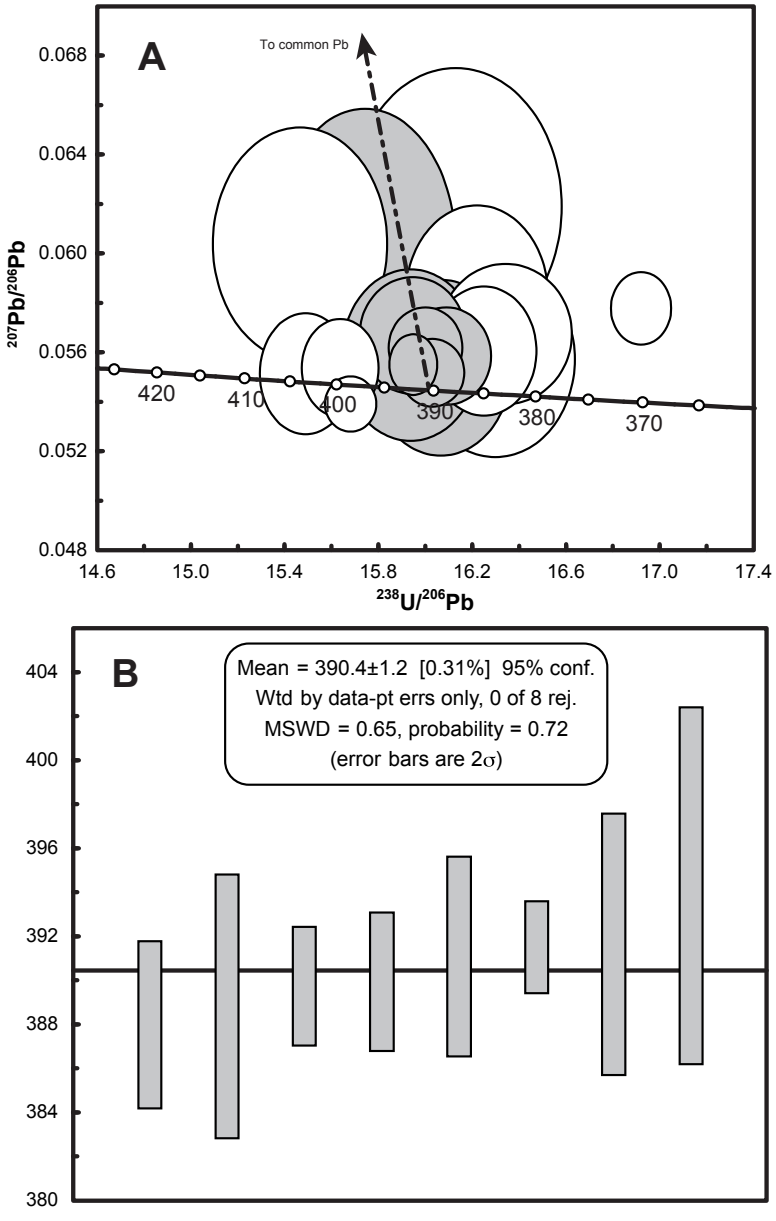

https://doi.org/10.5194/se-2020-53
Preprint. Discussion started: 14 May 2020
© Author(s) 2020. CC BY 4.0 License.

Solid Earth
Discussions
Open Access
EGU

Figure 4

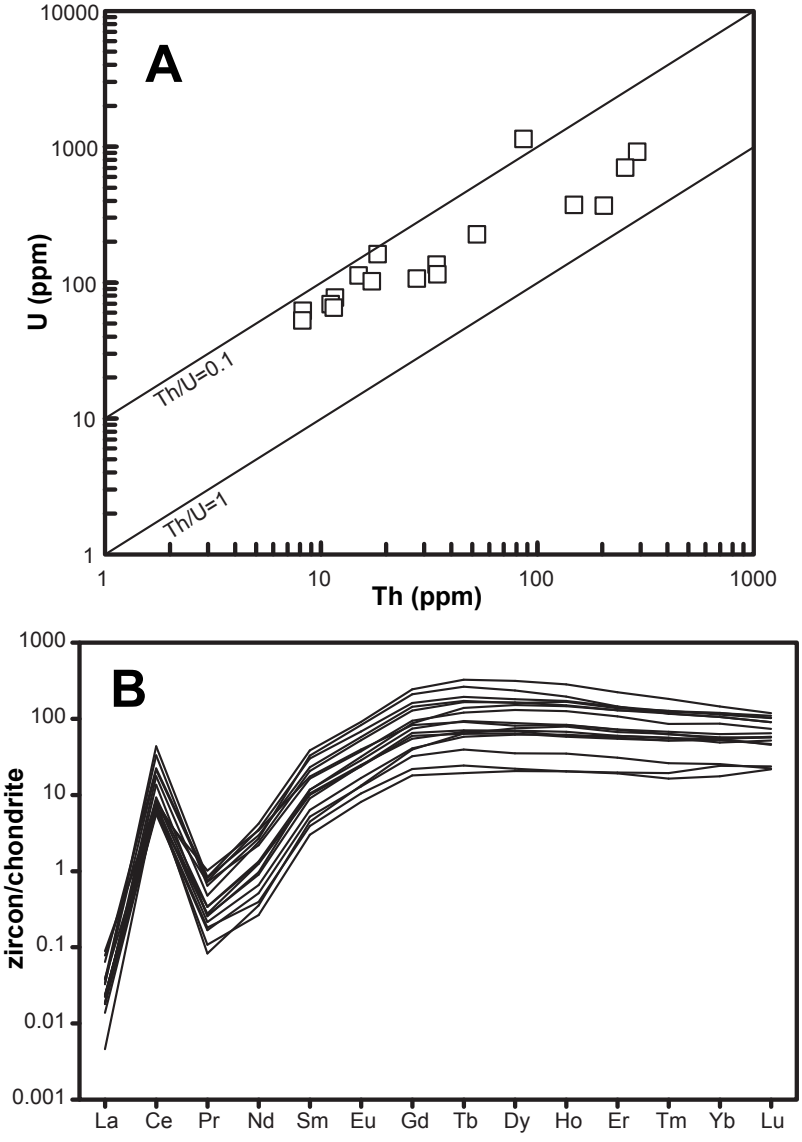

https://doi.org/10.5194/se-2020-53
Preprint. Discussion started: 14 May 2020
© Author(s) 2020. CC BY 4.0 License.

Solid Earth
Discussions
Open Access
EGU

Figure 5

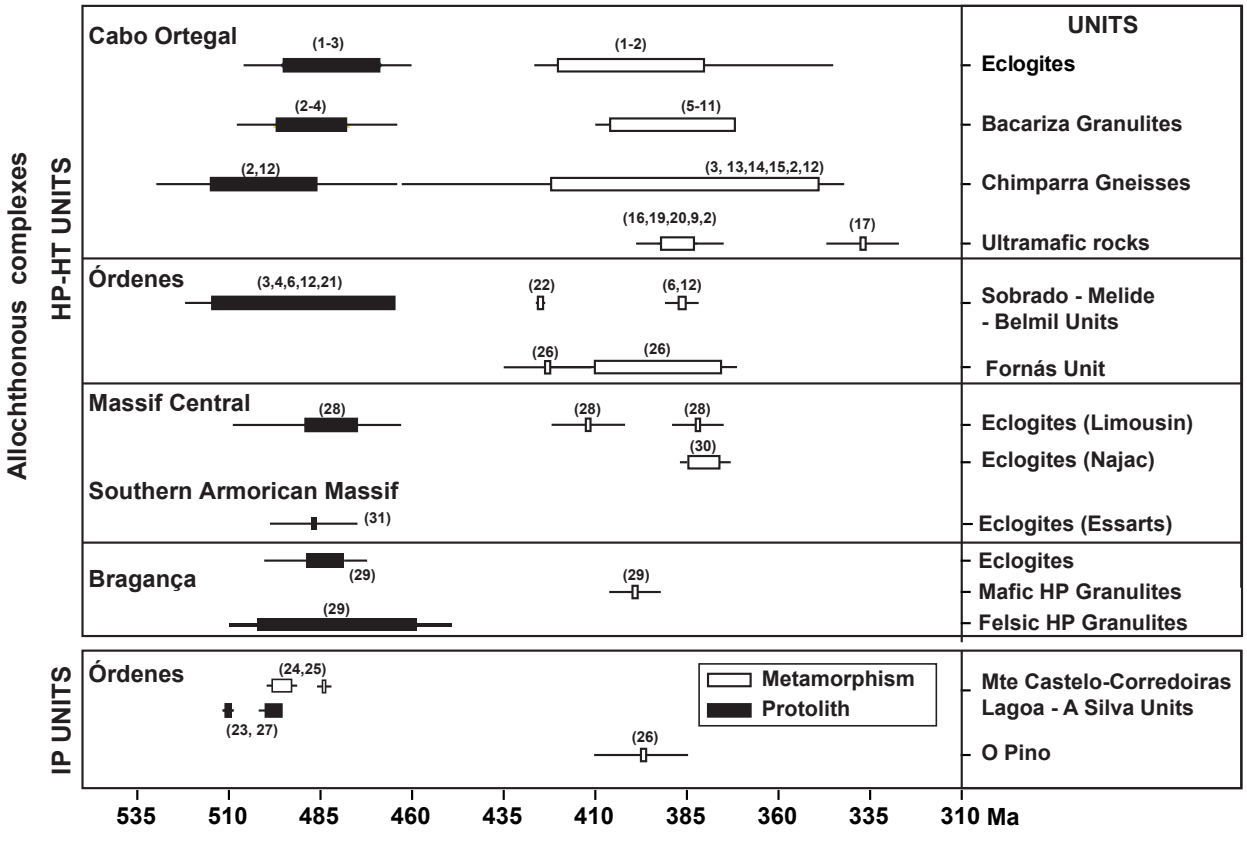

Abati et al. 1999, U/Pb: (23) Zrn; (24) Mnz
Berger et al. 2010, LA-ICP-MS: (28) Zrn
Bernard-Griffiths et al. 1985, U/Pb: (1) Zrn
Castiñeiras et al. 2010, SHRIMP: (25) Zrn
Dallmeyer & Tucker 1993, U/Pb: (27) Zrn
Dallmeyer et al. 1997, Ar/Ar: (22) Hbl
Fernánez Suárez et al. 2002, TIMS: (4) Zrn; (7) Ttn; (8) Rt; (12) Mnz
Fernández Suárez et al. 2007, SIMS: (6) Zrn
Gómez Barreiro et al. 2006, Ar/Ar: (26) Hbl
Kuijper et al. 1982, U/Pb: (21) Zrn Mnz
Lotout et al. 2018 LC-ICP-MS: (30), U-Pb_Zrn; Lu-Hf_Grt ; Sm-Nd_Grt
Mateus et al. 2016, SHRIMP: (29) Zrn
Ordóñez Casado et al. 2001, SHRIMP: (2) Zrn
Peucat et al. 1990, U/Pb: (3) Zrn; (5) Ar/Ar: Am; (13) Rb/Sr: Ms WR; (14) Rb/Sr: Bt WR
Peucat et al. 2017; LA-ICP-MS: (31) Zrn
Santos et al. 1996, U/Pb: (9) Zrn; (10) Ttn; (11) Ep; (19) Mnz; (20) Rt
Valverde Vaquero & Fernández, U/Pb: (15) Rt
Van Calsteren et al. 1979, Rb/Sr:(16) Phl (rcl); (17) Ed (rcl)